ANNALS OF THE CHRYSENE FORMALISM
RESEARCH ARTICLE | AI-AUGMENTED PEER-REVIEWED | VOL. 1, NO. 1 | SEPTEMBER 2026

Robust Geometric Confinement of Apoptotic Signaling Pathways: Bridging Stochastic Differential Equations and the Chrysene Formalism via H_∞-Inspired Molecular Splinting

Charles D. Schaper, Ph.D.
Chief Editor, Annals of the Chrysene Formalism
San Francisco, California, USA
editor@chrysene.com

Abstract

Classical pharmacology often represents cellular apoptosis as a stochastic dynamical system governed by noise-induced transitions within biochemical cascades. These systems can be modeled using stochastic differential equations (SDEs) to capture thermodynamic fluctuations, conformational drift, and solvent-mediated perturbations in the intracellular environment. Classical computer-aided drug design (CADD) typically optimizes ligand-target interactions through thermodynamic binding models, empirical force fields, molecular docking, molecular dynamics, and statistical sampling of conformational ensembles [TO10, KM02, LL16]. These methods are powerful, but they may not directly address the problem of robustly confining a target protein to a prescribed conformational neighborhood under persistent stochastic forcing.

This paper develops a mathematical framework for **robust geometric confinement** under the Chrysene Formalism. Instead of treating a molecular therapeutic as a time-dependent active controller, we model a rigid chrysene-based molecular brace as a passive static potential field or geometric constraint. The stochastic conformation of an apoptotic target protein is represented by a state vector $X_t \in \mathbb{R}^n$, and its deviation from a desired target conformation $X^* \in \mathcal{I}_C$ is measured by the Entropic Strain Tensor $E_{\text{drift}} = (X_t - X^*)(X_t - X^*)^T$, whose trace is the quadratic deviation $\text{Tr}(E_{\text{drift}}) = \|X_t - X^*\|^2$. An H_∞-inspired minimax formulation is used as a design principle for selecting static splinting potentials that reduce worst-case conformational strain under bounded perturbations, while residual Brownian noise is retained as an irreducible stochastic input. In the reflected-SDE idealization, a rigid geometric brace confines the trajectory to a compact tether domain of radius r_{tol}, yielding the pathwise bound $\|X_t - X^*\| \leq r_{\text{tol}}$. Thus, the principal mathematical result is finite-radius stochastic confinement. Exact zero strain arises only in the singular mathematical limit $r_{\text{tol}} \to 0$, not as a literal physical claim for thermally fluctuating molecular systems.

Keywords: Molecular splinting,Stochastic differential equations, H_∞ robust control, Apoptotic signaling pathways, Conformational stabilization, Entropic strain tensor, Reflected Brownian motion, Chrysene Formalism.

1 Introduction

The regulation of cellular apoptosis—the programmed sequence of events leading to cell death—stands as a central pillar of modern oncology, immunology, and regenerative medicine. Historically, the biochemical cascades governing apoptosis, such as the oligomerization of Bax/Bak on the outer mitochondrial membrane or the activation of the apoptosome via Caspase-9, have been conceptualized as stochastic dynamical systems. In the crowded, highly fluctuating aqueous environment of the cytoplasm, biomolecular conformations are subjected to continuous thermal bombardment. Classical pharmacology attempts to intervene in these pathways using small-molecule inhibitors or biological therapeutics designed to bind specific active sites.

Under the Chrysene Formalism, the proposed therapeutic mechanism is not a microscopic servo-controller and not an arbitrary time-dependent feedback actuator. Rather, a rigid, C_{2h}-symmetric aromatic backing plate (B_{plate}) is modeled as a passive geometric splint that alters the effective potential landscape and confines the target conformation to a finite neighborhood of a desired state. The physical restriction of the target's configuration

Citation: Schaper, C. D. (2026). Robust Geometric Confinement of Apoptotic Signaling Pathways: Bridging Stochastic Differential Equations and the Chrysene Formalism via H_∞-Inspired Molecular Splinting. *Annals of the Chrysene Formalism*, 1(1), 332–341. • © 2026 Charles D. Schaper. Distributed under the Creative Commons Attribution 4.0 International License (CC BY 4.0). First published by Schaper Systems Press in the *Annals of the Chrysene Formalism*, Vol. 1, No. 1 (2026).

space to a compact domain Ω enforces a Kinematic Tether Limit r_{tol}, which should be interpreted as a finite conformational tolerance rather than a literal zero-radius constraint.

To mathematically capture the unconstrained fluctuations, we model the apoptotic target conformation $X_t \in \mathbb{R}^n$ using a multidimensional Itô stochastic differential equation:

$$dX_t = f(X_t)\,dt + g(X_t)\,dW_t + u_t\,dt, \tag{1}$$

where $f(X_t) \in \mathbb{R}^n$ represents intrinsic folding drift driven by the protein's potential landscape, $g(X_t) \in \mathbb{R}^{n\times m}$ is the diffusion matrix representing stochastic thermodynamic perturbations of the solvated state, and $W_t \in \mathbb{R}^m$ is a standard multidimensional Brownian motion. Throughout this manuscript, $g(X)$ denotes the diffusion coefficient of the stochastic dynamics; when the simulation section uses the scalar parameter σ, it refers only to the numerical noise intensity used in the toy example. The term u_t is interpreted differently in the present framework than in classical active feedback control. For a passive molecular brace, the physically admissible structural influence is a static potential gradient:

$$u_t = -\nabla\Psi_{\text{splint}}(X_t). \tag{2}$$

This paper introduces the Chrysene Formalism [Sch26b] as a theoretical framework for geometry-driven conformational stabilization. Rather than claiming the literal elimination of thermal motion, the model seeks to bound conformational excursions within a prescribed tether domain. The desired conformation is represented by $X^* \in \mathcal{I}_C$, where $\mathcal{I}_C$ denotes an idealized discrete algebraic manifold of target conformations.

To bridge continuous stochastic dynamics with the discrete target manifold, we define the Entropic Strain Tensor:

$$E_{\text{drift}} = (X_t - X^*)(X_t - X^*)^T. \tag{3}$$

Taking the trace gives the scalar quadratic deviation

$$\text{Tr}(E_{\text{drift}}) = \|X_t - X^*\|^2. \tag{4}$$

The revised control objective is therefore not to force stochastic drift identically to zero in a physical system, but to reduce and bound the strain within a finite tether neighborhood.

Using an H_∞-inspired minimax design principle, we formulate the structural design problem as the selection of a static splinting potential that reduces worst-case entropic strain under bounded adversarial perturbations while retaining Brownian forcing as residual stochastic noise. Brownian motion is not treated as a directly maximized control input. Instead, we distinguish the deterministic adversarial disturbance v_t from the stochastic Brownian term dW_t. A design-stage objective may therefore be written as

$$\inf_{\Psi_{\text{splint}}} \sup_{v} \mathbb{E}\left[\int_0^T \left(\text{Tr}(E_{\text{drift}}(t)) + \|\nabla\Psi_{\text{splint}}(X_t)\|_R^2 - \gamma^2\|v_t\|^2\right) dt\right], \tag{5}$$

where R is a positive-definite weighting matrix, $\gamma > 0$ is the prescribed disturbance attenuation level, and v_t is an energy-bounded deterministic perturbation used in the robust design problem. The Brownian term remains part of the stochastic dynamics and represents irreducible thermodynamic fluctuation.

The physical realization of this mathematical design objective is not a flexible, classical small molecule, but a proposed rigid tetrasubstituted chrysene brace compiled via the Abiotic Loom Software Development Kit (SDK) [Sch26a]. Chrysene, a polycyclic aromatic hydrocarbon consisting of four fused benzene rings, provides a rigid planar scaffold. By appending functional groups at selected vector positions, the model proposes a molecular splint that biases or confines the target protein toward a desired conformational state. This is best interpreted as robust finite-radius conformational stabilization rather than absolute deterministic control over an entire cellular apoptotic pathway.

1.1 Hypothesis

We hypothesize that stochastic fluctuations of selected apoptotic target proteins can be parameterized by the Entropic Strain Tensor and reduced through static potential landscape engineering. Within the Chrysene Formalism, a rigid tetrasubstituted chrysene brace is modeled as an artificial potential or geometric boundary that confines the target conformation to a finite tether neighborhood of a desired state $X^* \in \mathcal{I}_C$. The expected result is robust conformational stabilization and bounded stochastic drift, with exact zero strain appearing only as an idealized mathematical limit.

2 Theoretical Framework

The mathematical bridge between stochastic protein dynamics and molecular splinting requires three elements: a stochastic state model, a strain measure, and a physically admissible class of static molecular interventions. The stochastic state model describes how the target protein moves under native drift and thermodynamic noise. The strain measure quantifies deviation from a desired conformation. The admissible intervention class represents the fact that a passive molecular brace can implement static potential gradients or geometric boundaries, but not arbitrary dynamic feedback.

2.1 Stochastic Dynamics of Apoptotic Signaling Pathways

We model the unconstrained conformational state of an apoptotic target protein or protein complex, denoted by the state vector $X_t \in \mathbb{R}^n$, as

$$dX_t = f(X_t)\,dt + g(X_t)\,dW_t + u_t\,dt, \tag{6}$$

where:

- $f(X_t) \in \mathbb{R}^n$ represents intrinsic conservative folding drift derived from the native potential landscape, with $f(X_t) = -\nabla\Phi(X_t)$ when $\Phi : \mathbb{R}^n \to \mathbb{R}$ is a potential.
- $g(X_t) \in \mathbb{R}^{n\times m}$ represents the diffusion tensor characterizing stochastic thermodynamic perturbations of the solvated aqueous environment.
- W_t is an m-dimensional standard Brownian motion.
- $u_t \in \mathbb{R}^n$ historically represents an active control input. In the Chrysene Formalism, a physically realized passive brace is instead represented by the static conservative field $u_t = -\nabla\Psi_{\text{splint}}(X_t)$.

Consequently, the SDE under geometric splinting becomes

$$dX_t = -\nabla\big(\Phi(X_t) + \Psi_{\text{splint}}(X_t)\big)\,dt + g(X_t)\,dW_t. \tag{7}$$

The Brownian term remains present. The proposed splint modifies the drift and may confine the stochastic process to a bounded region when appropriate stability or reflection conditions hold.

2.2 The Entropic Strain Tensor and Pathological Graphs

To quantify deviation from a therapeutic conformation, define

$$E_{\text{drift}} = (X_t - X^*)(X_t - X^*)^T, \tag{8}$$

where $X^* \in \mathcal{I}_C \subset \mathbb{R}^n$ is the target coordinate vector. Since

$$\text{Tr}(E_{\text{drift}}) = \|X_t - X^*\|^2, \tag{9}$$

the trace provides a scalar quadratic measure of conformational strain.

To scale this representation to a network of constrained coordinates, define the Pathological Graph $G_{\text{path}} = (V, E)$ [Sch26c], where vertices V represent selected domain coordinates and edges E represent physical or topological constraints. For example, vertices may correspond to selected residue positions, domain centroids, hinge regions, inter-residue distances, reaction coordinates, or conformational landmarks, while edges encode geometric or functional relationships among those landmarks. The static correction field is

$$\vec{V}_{\text{corr}}(X_t) = -\nabla\Psi_{\text{splint}}(X_t). \tag{10}$$

The Global Entropic Strain Tensor is

$$E_{\text{global}} = \sum_{i\in V}(X_i - X_i^*)(X_i - X_i^*)^T. \tag{11}$$

Theorem 1 (Finite-Radius Pathological Re-stabilization)**.** *Let $G_{\text{path}} = (V, E)$ be a pathological graph whose vertices represent selected conformational coordinates of the target. Suppose the application of a static splinting potential Ψ_{splint} confines each vertex $i \in V$ to a local tether neighborhood*

$$\|X_i(t) - X_i^*\| \le r_{\text{tol},i}$$

for all $t \ge 0$, almost surely. Then the global entropic strain satisfies the finite-radius bound

$$\text{Tr}(E_{\text{global}}(t)) \le \sum_{i\in V} r_{\text{tol},i}^2 \quad \textit{for all } t \ge 0 \quad \textit{a.s.} \tag{12}$$

In the singular idealization $r_{\text{tol},i} \to 0$ for every $i \in V$, the bound collapses to zero.

Proof. By definition,

$$E_{\text{global}}(t) = \sum_{i\in V}(X_i(t) - X_i^*)(X_i(t) - X_i^*)^T. \tag{13}$$

Taking the trace gives

$$\begin{aligned}\text{Tr}(E_{\text{global}}(t)) &= \sum_{i\in V}\text{Tr}\left((X_i(t) - X_i^*)(X_i(t) - X_i^*)^T\right)\\ &= \sum_{i\in V}\|X_i(t) - X_i^*\|^2.\end{aligned} \tag{14}$$

Using the local tether assumption $\|X_i(t) - X_i^*\| \le r_{\text{tol},i}$, we obtain

$$\text{Tr}(E_{\text{global}}(t)) \le \sum_{i\in V} r_{\text{tol},i}^2. \tag{15}$$

If $r_{\text{tol},i} \to 0$ for every vertex, then the right-hand side tends to zero. For physical molecular systems, however, the finite-radius bound is the operative conclusion. □

2.3 The H_∞ Minimax Robust Control Formulation

Because the physical intervention is a static brace, the H_∞ optimization is re-contextualized from real-time feedback control to computational shape and parameter optimization during the design phase. The optimization problem is formulated over the design space of the artificial potential rather than a temporal input:

$$\inf_{\Psi_{\text{splint}}}\sup_{v}\mathbb{E}\left[\int_0^T\left(\text{Tr}(E_{\text{drift}}(t)) + \|\nabla\Psi_{\text{splint}}(X_t)\|_R^2 - \gamma^2\|v_t\|^2\right)dt\right]. \tag{16}$$

Here v_t is an energy-bounded deterministic worst-case perturbation used in the H_∞ design problem. It is distinct from the Brownian motion W_t. The Brownian term remains in the stochastic dynamics as residual thermodynamic noise, while v_t represents the adversarial disturbance in the minimax formulation.

In the context of the Abiotic Loom SDK, this minimax condition is evaluated during the compilation phase to identify

large admissible perturbations Δ_{ent} and calculate the structural stability of the geometry K under those perturbations:

$$K_{\text{opt}} = \arg\min_{K} \max_{\Delta_{\text{ent}}} \|\mathcal{T}(K, \Delta_{\text{ent}})\| . \tag{17}$$

This formulation is best read as a structural robustness criterion for the compiled brace, not as a claim that the molecule performs arbitrary active feedback control.

2.4 Computational Tractability and Effective Design-Space Reduction

A fundamental mathematical challenge in evaluating nonlinear H_∞ optimal control for biological macromolecules is the curse of dimensionality. Classically, the state vector $X_t \in \mathbb{R}^n$ of a solvated protein may possess thousands of degrees of freedom, and the unconstrained conformational search space can grow exponentially.

The Chrysene Formalism proposes to reduce the effective design space through strict geometric restriction. Rather than computing over the unbounded continuum $\mathbb{R}^n$, the evaluation is restricted to a finite or lower-dimensional class of geometrically admissible configurations on the idealized $\mathcal{I}_C$ manifold. The C_{2h}-symmetric 3,6,9,12-tetrasubstituted chrysene lattice acts as an algebraic and geometric filter [Sch26a].

A formal claim of polynomial complexity would require an explicit algorithm, input-size definition, branching-factor estimate, and proof. In the absence of that algorithmic proof, the appropriate claim is that the proposed geometric restriction reduces the effective design space relative to unconstrained macromolecular search. A rigorous complexity theorem is left for future work.

2.5 The Chrysene Formalism and Geometric Splinting

The physical realization of the robust structural design is modeled as a rigid, C_{2h}-symmetric, tetrasubstituted chrysene brace compiled via the Abiotic Loom SDK. The Chrysene Formalism utilizes an Aromatic Backing Plate (B_{plate}) to act as a physical orthotic brace.

The B_{plate} is instantiated as a discrete, C_{2h}-symmetric 3,6,9,12-tetrasubstituted chrysene core. This rigid aromatic scaffold mechanically enforces the Kinematic Tether Limit r_{tol}, which defines the maximum allowable coarse-grained spatial deviation of the target:

$$\|X_t - X^*\| \leq r_{\text{tol}}. \tag{18}$$

By restricting the target's configuration space to a compact domain Ω, the splint enforces a finite bound on conformational strain. Therefore,

$$\text{Tr}(E_{\text{drift}}(t)) \leq r_{\text{tol}}^2. \tag{19}$$

Through this geometric splinting, stochastic trajectories are bounded within a tether domain. The model supports robust conformational stabilization of selected target states, not literal elimination of thermal motion or absolute control of an entire cellular pathway.

2.6 Biophysical Interpretation and Model Scope

The state vector X_t should be interpreted as a coarse-grained conformational coordinate vector, not as a complete atomistic representation of the target protein. Depending on the application, its components may represent selected residue positions, domain centroids, inter-residue distances, reaction coordinates, principal conformational modes, or other reduced structural descriptors. The target state X^* represents a desired coarse-grained conformation or conformational neighborhood rather than a perfectly fixed atomic structure.

Similarly, the vertices V of the pathological graph $G_{\text{path}} = (V, E)$ represent selected conformational landmarks. For example, in a Bax/Bak-like or caspase-like setting, vertices could correspond to domain centroids, hinge regions, interface residues, loop positions, or other structural features relevant to activation or inhibition. The edges E represent geometric, steric, or functional relationships among those landmarks.

The present manuscript does not claim to establish a validated atomistic binding pose, binding affinity, target selectivity, intracellular delivery, pharmacokinetics, toxicity profile, or pathway-level control of apoptosis. Those questions require molecular docking or molecular dynamics, synthetic feasibility analysis, biochemical binding assays, cellular assays, and ultimately experimental validation [KM02, TO10]. The purpose of the present work is narrower: to formulate a mathematical framework in which a rigid molecular splint can be idealized as a static potential or reflected-SDE boundary that confines coarse-grained conformational excursions within a finite tether radius.

3 Mathematical Expansion and Proofs

This section develops a mathematical foundation for robust finite-radius confinement of stochastic conformational dynamics. Let $(\Omega_p, \mathcal{F}, \{\mathcal{F}_t\}_{t\geq 0}, \mathbb{P})$ be a filtered probability space satisfying the usual conditions and supporting the m-dimensional standard Brownian motion W_t. The state space of the target protein is denoted by $\mathcal{X} \subseteq \mathbb{R}^n$.

3.1 Hamilton-Jacobi-Isaacs (HJI) Formulation of the Minimax Game

For the purpose of deriving the HJI variational inequality, we first maintain the generalized control variable u_t, while recognizing that physical molecular realization requires $u_t = -\nabla\Psi_{\text{splint}}(X_t)$.

Define $\widetilde{X}_t = X_t - X^*$. The running cost is

$$L(X_t, u_t, v_t) = \widetilde{X}_t^T Q \widetilde{X}_t + u_t^T R u_t - \gamma^2 \|v_t\|^2. \tag{20}$$

Here $v_t \in \mathbb{R}^m$ represents an energy-bounded deterministic worst-case perturbation used in the H_∞ design problem. It is distinct from the Brownian motion W_t. The Brownian term remains in the stochastic dynamics as residual thermodynamic noise.

The value function is formally defined by

$$V(X) = \min_u \max_v \mathbb{E}\left[\int_0^\infty e^{-\beta t} L(X_t, u_t, v_t)\, dt \,\middle|\, X_0 = X\right], \tag{21}$$

where $\beta > 0$. The corresponding HJI equation is

$$\begin{aligned}\beta V(X) = \min_{u\in\mathbb{R}^n} \max_{v\in\mathbb{R}^m} \Big\{ & \nabla V(X)^T \big(f(X) + u + g(X)v\big) \\ & + \frac{1}{2}\operatorname{Tr}\big(g(X)g(X)^T \nabla^2 V(X)\big) + \widetilde{X}^T Q \widetilde{X} \\ & + u^T R u - \gamma^2 \|v\|^2 \Big\}. \end{aligned} \tag{22}$$

Scope of the HJI formulation. The Hamilton–Jacobi–Isaacs equation above is used here as a formal design equation for comparing idealized stabilizing vector fields under worst-case deterministic perturbations [BB95]. We do not prove global existence, uniqueness, or smoothness of the value function V, nor do we prove global solvability of the nonlinear HJI equation over the full macromolecular state space. These analytical questions are nontrivial and depend on the admissible control class, compactness of the design space, regularity of f and g, boundary behavior, and coercivity of the running cost. In the present work, the HJI formulation should therefore be interpreted as an H_∞-inspired design principle rather than a complete global optimal-control theorem.

Lemma 2 (Saddle-Point Controller and Disturbance Policies)**.** *The formal unrestricted feedback saddle-point policies are*

$$u^*(X) = -\frac{1}{2} R^{-1} \nabla V(X), \tag{23}$$

$$v^*(X) = \frac{1}{2\gamma^2} g(X)^T \nabla V(X). \tag{24}$$

Proof. The Hamiltonian is strictly convex in u and strictly concave in v. The first-order condition with respect to u gives

$$\nabla V(X) + 2Ru = 0, \tag{25}$$

so

$$u^*(X) = -\frac{1}{2} R^{-1} \nabla V(X). \tag{26}$$

The first-order condition with respect to v gives

$$g(X)^T \nabla V(X) - 2\gamma^2 v = 0, \tag{27}$$

so

$$v^*(X) = \frac{1}{2\gamma^2} g(X)^T \nabla V(X). \tag{28}$$

□

3.2 Potential-Restricted Molecular Realizability

A synthesized molecular brace cannot implement an arbitrary time-dependent feedback law. The unrestricted feedback field

$$u^*(X) = -\frac{1}{2} R^{-1} \nabla V(X)$$

is physically realizable by a passive molecular splint only when it can be represented, at least locally, as a conservative gradient field

$$u^*(X) = -\nabla \Psi(X).$$

Accordingly, the molecular design problem is not the unrestricted HJI feedback problem. It is a potential-restricted approximation problem: find an admissible, chemically realizable static potential $\Psi_{\text{splint}} \in \mathcal{A}_\Psi$ such that

$$-\nabla \Psi_{\text{splint}}(X)$$

approximates a desired stabilizing vector field over the conformational region of interest. The set $\mathcal{A}_\Psi$ represents geometric, chemical, steric, and synthetic constraints imposed by the chrysene scaffold and its substituents. The H_∞ equations therefore provide a benchmark for robust stabilization, while the physically relevant design task is the construction of static molecular geometries whose induced potential gradients approximate that benchmark within the tether domain.

3.3 Stochastic Variance Bounding under Static Splinting

The HJI formalism gives a robust design principle, but pointwise stochastic stabilization requires a Lyapunov condition. We state this condition explicitly, following standard stochastic Lyapunov stability reasoning [Kha12].

Assumption 1 (Local Stochastic Stabilization)**.** *There exists a twice continuously differentiable Lyapunov function $V : \mathbb{R}^n \to \mathbb{R}_+$ and constants $a > 0$, $\theta \geq 0$, $c_1 > 0$, and $c_2 > 0$ such that, near X^*,*

$$c_1 \|X - X^*\|^2 \leq V(X) \leq c_2 \|X - X^*\|^2, \tag{29}$$

and the infinitesimal generator $\mathcal{L}^\Psi$ of the splinted stochastic dynamics satisfies

$$\mathcal{L}^\Psi V(X) \leq -aV(X) + \theta. \tag{30}$$

Theorem 3 (Ultimate Mean-Square Boundedness)**.** *Under the local stochastic stabilization assumption,*

$$\mathbb{E}[V(X_t)] \le e^{-at}V(X_0) + \frac{\theta}{a}(1 - e^{-at}). \tag{31}$$

Consequently,

$$\mathbb{E}[\mathrm{Tr}(E_{\mathrm{drift}}(t))] \le \frac{e^{-at}V(X_0)}{c_1} + \frac{\theta}{ac_1}(1 - e^{-at}), \tag{32}$$

and

$$\limsup_{t\to\infty} \mathbb{E}[\mathrm{Tr}(E_{\mathrm{drift}}(t))] \le \frac{\theta}{ac_1}. \tag{33}$$

Proof. Dynkin's formula applied to $e^{at}V(X_t)$ gives

$$\mathbb{E}[e^{at}V(X_t)] = V(X_0) + \mathbb{E}\left[\int_0^t e^{as}\left(aV(X_s) + \mathcal{L}^{\Psi}V(X_s)\right) ds\right]. \tag{34}$$

Using $\mathcal{L}^{\Psi}V(X) \le -aV(X) + \theta$, we obtain

$$\mathbb{E}[e^{at}V(X_t)] \le V(X_0) + \int_0^t e^{as}\theta\, ds = V(X_0) + \frac{\theta}{a}(e^{at} - 1). \tag{35}$$

Multiplying by e^{-at} yields

$$\mathbb{E}[V(X_t)] \le e^{-at}V(X_0) + \frac{\theta}{a}(1 - e^{-at}). \tag{36}$$

Since $c_1\|X_t - X^*\|^2 \le V(X_t)$ and $\mathrm{Tr}(E_{\mathrm{drift}}(t)) = \|X_t - X^*\|^2$, the strain bound follows. □

3.4 Rigorous Analysis of Geometric Splinting via Reflected SDEs

To unify the potential-field model with hard geometric confinement, we idealize the stiff limit of Ψ_{splint} as a reflecting boundary, following the standard reflected-SDE/Skorokhod framework [LS84]. Let the configuration space be the compact, closed domain

$$\Omega = \{X \in \mathbb{R}^n \mid \|X - X^*\| \le r_{\mathrm{tol}}\}. \tag{37}$$

The constrained dynamics are modeled by the reflected SDE

$$dX_t = f(X_t)\, dt + g(X_t)\, dW_t + u_t\, dt - \nu(X_t)\, dK_t, \tag{38}$$

where $\nu(X)$ is the outward unit normal on $\partial\Omega$, and K_t is the non-decreasing boundary local-time process satisfying

$$K_t = \int_0^t \mathbb{I}_{\{X_s \in \partial\Omega\}}\, dK_s. \tag{39}$$

Theorem 4 (Bounded Brownian Excursions under Geometric Reflection)**.** *Let the target protein be constrained by the rigid B_{plate} defining the compact domain*

$$\Omega = \{X \in \mathbb{R}^n : \|X - X^*\| \le r_{\mathrm{tol}}\}.$$

Assume the reflected SDE is well posed on Ω. Then

$$\|X_t - X^*\| \le r_{\mathrm{tol}} \quad \textit{for all } t \ge 0 \quad \textit{a.s.} \tag{40}$$

Consequently,

$$\mathrm{Tr}(E_{\mathrm{drift}}(t)) \le r_{\mathrm{tol}}^2 \quad \textit{for all } t \ge 0 \quad \textit{a.s.} \tag{41}$$

Moreover,

$$\lim_{r_{\mathrm{tol}}\to 0} \mathbb{E}\left[\sup_{t\ge 0} \|X_t - X^*\|^2\right] = 0. \tag{42}$$

Proof. By construction of the reflected process, $X_t \in \Omega$ for all $t \ge 0$ almost surely. Therefore,

$$\|X_t - X^*\| \le r_{\mathrm{tol}} \quad \text{for all } t \ge 0 \quad \text{a.s.} \tag{43}$$

Squaring both sides gives

$$\|X_t - X^*\|^2 \le r_{\mathrm{tol}}^2. \tag{44}$$

Since $\mathrm{Tr}(E_{\mathrm{drift}}(t)) = \|X_t - X^*\|^2$, the finite-radius strain bound follows. Taking the supremum over time and expectation gives

$$\mathbb{E}\left[\sup_{t\ge 0} \|X_t - X^*\|^2\right] \le r_{\mathrm{tol}}^2. \tag{45}$$

Letting $r_{\mathrm{tol}} \to 0$ yields the stated singular-limit result. □

To interpret the boundary term, apply Itô's formula to $U(X_t) = \frac{1}{2}\|X_t - X^*\|^2$:

$$dU(X_t) = (X_t - X^*)^T(f(X_t) + u_t)\, dt + \frac{1}{2}\,\mathrm{Tr}\left(g(X_t)g(X_t)^T\right) dt + (X_t - X^*)^T g(X_t)\, dW_t - (X_t - X^*)^T \nu(X_t)\, dK_t. \tag{46}$$

On the boundary, $X_t - X^* = r_{\mathrm{tol}}\nu(X_t)$, so the reflection term is $r_{\mathrm{tol}}\, dK_t$. Thus, the reflected-SDE model proves finite-radius confinement for every positive r_{tol}. The Brownian component is not literally eliminated inside the tether region; rather, Brownian excursions are prevented from leaving the compact domain. Exact zero variance appears only in the singular idealization $r_{\mathrm{tol}} \to 0$.

3.5 Thermodynamic Reality of the Kinematic Tether Limit

The mathematical limit $r_{\mathrm{tol}} \to 0$ is useful as an idealization, but a real molecular brace has finite stiffness, finite binding

energy, finite solvation effects, and nonzero thermal vibration. Therefore, the physically meaningful tether radius is positive.

Because the Aromatic Backing Plate (B_{plate}) relies on a rigid tetrasubstituted chrysene scaffold ($C_{18}H_{12}$), its binding energetics may include enthalpic contacts, desolvation penalties, hydrophobic collapse, and conformational entropy changes. A schematic thermodynamic payload can be written as

$$\Delta G_{\text{payload}} = \Delta H_{\text{bind}} - T\Delta S_{\text{solv}} + \Delta G_{\text{desolv}} + \Delta G_{\text{conf}}. \tag{47}$$

Rather than adding the magnitude of $\Delta G_{\text{payload}}$ directly to the radius, it is more consistent to model the splint as increasing the effective stiffness:

$$\kappa_{\text{eff}} = \kappa_{\text{native}} + \kappa_{\text{splint}}(\Delta G_{\text{payload}}, \text{geometry}). \tag{48}$$

A phenomenological thermal fluctuation scale can then be written as

$$r_{\text{tol}} \approx r_{\text{base}} + \sqrt{\frac{k_B T}{\kappa_{\text{eff}}}}, \tag{49}$$

where k_B is Boltzmann's constant, T is temperature, and r_{base} is irreducible baseline vibration or coordinate uncertainty. In this form, increasing the effective stiffness decreases the thermal fluctuation radius, which is consistent with the intended confinement mechanism. Thus, the physical conclusion is finite-radius confinement rather than literal cessation of atomic vibration.

3.6 Convergence of the Global Entropic Strain Tensor

We now extend the local boundary result to the pathological graph $G_{\text{path}} = (V, E)$.

Theorem 5 (Global Finite-Radius Strain Bound)**.** *Let*

$$E_{\text{global}}(t) = \sum_{i \in V} (X_i(t) - X_i^*)(X_i(t) - X_i^*)^T. \tag{50}$$

Assume that each vertex $i \in V$ is confined to a local tether radius $r_{\text{tol},i}$:

$$\|X_i(t) - X_i^*\| \le r_{\text{tol},i} \quad \textit{for all } t \ge 0 \quad \textit{a.s.} \tag{51}$$

Then

$$\operatorname{Tr}(E_{\text{global}}(t)) \le \sum_{i \in V} r_{\text{tol},i}^2 \quad \textit{for all } t \ge 0 \quad \textit{a.s.} \tag{52}$$

Proof. Taking the trace gives

$$\begin{aligned} \operatorname{Tr}(E_{\text{global}}(t)) &= \sum_{i \in V} \operatorname{Tr}\left((X_i(t) - X_i^*)(X_i(t) - X_i^*)^T \right) \\ &= \sum_{i \in V} \|X_i(t) - X_i^*\|^2. \end{aligned} \tag{53}$$

Using the local tether bounds,

$$\|X_i(t) - X_i^*\|^2 \le r_{\text{tol},i}^2. \tag{54}$$

Summing over $i \in V$ proves the result. □

Remark 1 (Idealized Zero-Strain Limit)**.** *If $r_{\text{tol},i} \to 0$ for every vertex, then the bound tends to zero. In physical molecular systems, however, the operative result is the finite bound*

$$\operatorname{Tr}(E_{\text{global}}(t)) \le \sum_{i \in V} r_{\text{tol},i}^2.$$

4 Simulation Results

To illustrate the mathematical framework, we simulated a high-dimensional stochastic system with a double-well potential, a static splinting potential, and a projected Euler-Maruyama confinement step. The simulation should be interpreted as a proof-of-concept demonstration of finite-radius confinement, not as a complete numerical solution of the H_∞ Hamilton-Jacobi-Isaacs equation. The projected Euler-Maruyama method first advances the unconstrained stochastic dynamics and then projects any state outside the tether domain back to the boundary, thereby approximating a reflected-SDE confinement mechanism.

The state vector $X_t \in \mathbb{R}^{10}$ represents ten coarse-grained spatial coordinates within an apoptotic domain. The intrinsic high-dimensional potential landscape is modeled as

$$\Phi(X) = \sum_{d=1}^{10} \frac{1}{4}(x_d^2 - 1)^2, \tag{55}$$

which yields stable local minima representing a pathological basin at

$$X_{\text{path}} = [-1.0, \ldots, -1.0]^T$$

and an ideal therapeutic conformation at

$$X^* = [1.0, \ldots, 1.0]^T.$$

The system is initialized at $X_0 = [-0.9, \ldots, -0.9]^T$. The thermal noise intensity is set to $\sigma = 0.30$. The intervention occurs at $T_{\text{control}} = 5.0$ s, when a static splinting potential is activated with restoring stiffness $k_{\text{splint}} = 25.0$ and tether radius $r_{\text{tol}} = 0.50$.

The numerical quantities reported below were computed directly from the simulated stochastic trajectory. They are included to explicitly highlight the diagnostics required to support the finite-radius confinement interpretation.

The table distinguishes visual illustration from quantitative validation. In particular, the maximum post-intervention deviation tests whether the simulated process remains within the prescribed tether scale, while the pre/post strain ratio quantifies the profound degree of stabilization produced by the static splinting potential in this illustrative model.

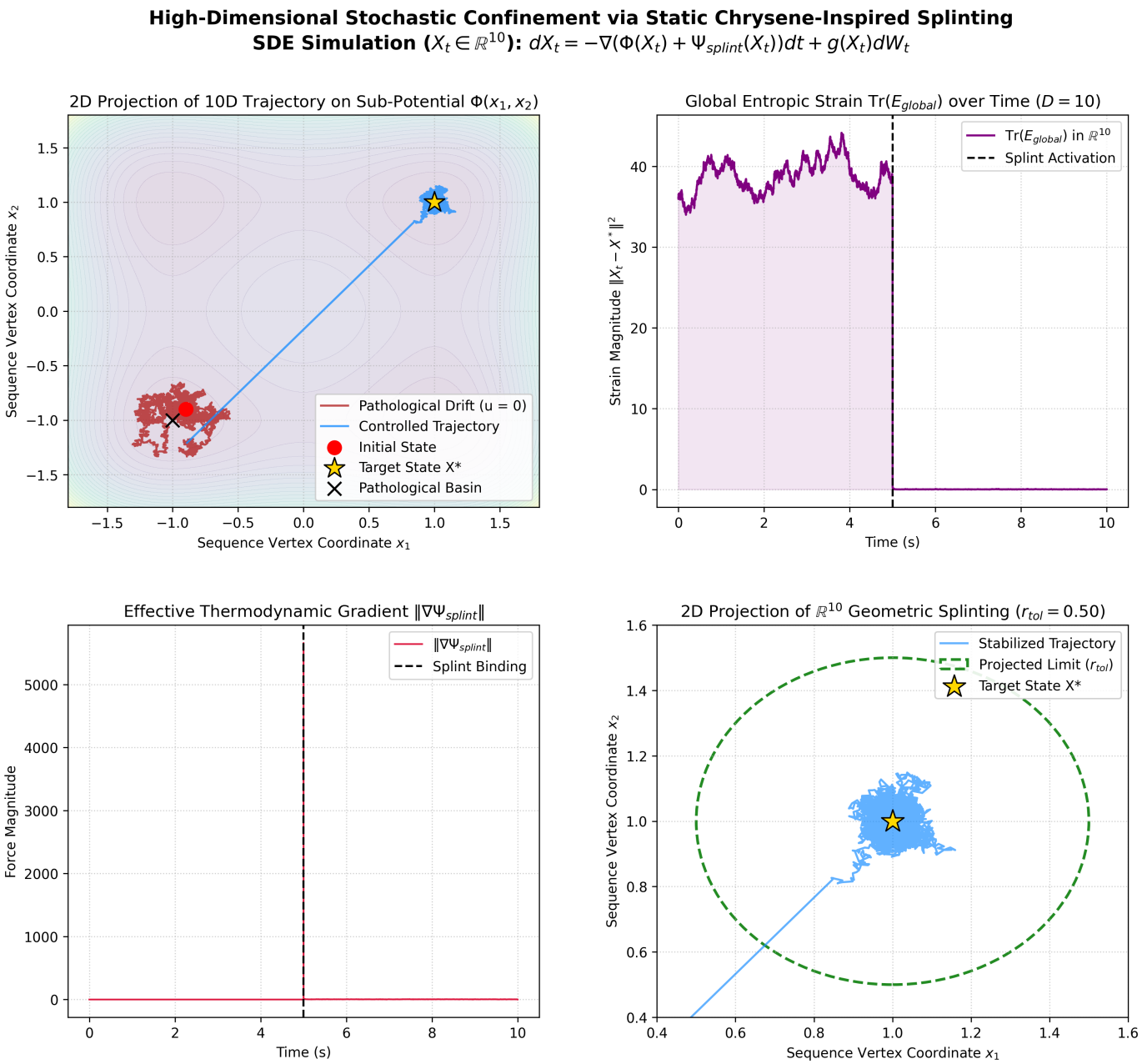


Figure 1: Illustrative high-dimensional stochastic confinement under a static chrysene-inspired splinting potential. **Panel A** illustrates a 2D projection of the conformational trajectory on the sub-potential landscape $\Phi(x_1, x_2)$. **Panel B** shows the temporal evolution of the global entropic strain $\mathrm{Tr}(E_{\mathrm{global}})$, which decreases after splint activation and remains bounded by the tether scale. **Panel C** depicts the computed magnitude of the restoring gradient $\|\nabla\Psi_{\mathrm{splint}}\|$ in the toy simulation; it is not a measured molecular force and does not represent mechanical work by an active motor. **Panel D** provides a zoomed-in 2D projection of the target state, demonstrating confinement within the projected kinematic tether limit $r_{\mathrm{tol}} = 0.50$.

Table 1: Quantitative diagnostics for the illustrative 10-dimensional confinement simulation.

Quantity	Value
Pre-intervention mean strain, $t < T_{\text{control}}$	$\langle \|\|X_t - X^*\|\|^2 \rangle_{\text{pre}} = 40.23$
Post-intervention mean strain, $t > T_{\text{control}}$	$\langle \|\|X_t - X^*\|\|^2 \rangle_{\text{post}} = 0.017$
Pre/post strain ratio	2366
Maximum post-intervention deviation	$\max_{t>T_{\text{control}}} \|\|X_t - X^*\|\| = 0.500$
Tether radius	$r_{\text{tol}} = 0.50$
Final strain	$\|\|X_T - X^*\|\|^2 = 0.015$
Maximum pre-projection tether violation	6.17

4.1 Conformational Trajectory on the Potential Landscape

Panel A of Figure 1 displays a two-dimensional projection of the $\mathbb{R}^{10}$ trajectory. Before intervention, the structural constraint is absent and the state remains near the pathological basin under native drift and stochastic forcing. After activation of the static splinting potential, the state is biased toward the desired conformation X^*. This illustrates potential-driven conformational stabilization, not elimination of all thermal motion.

4.2 Temporal Decay of the Global Entropic Strain

Panel B of Figure 1 tracks $\text{Tr}(E_{\text{global}}) = \|X_t - X^*\|^2$ within the simulation. After splint activation, the global strain decreases rapidly and then remains bounded by the tether scale. The correct interpretation is finite-radius confinement rather than proof of exact asymptotic zero strain in a physical molecular system.

4.3 Thermodynamic Binding Gradient and Elastic Restoring Force

Panel C of Figure 1 illustrates the magnitude of the effective thermodynamic gradient $\|\nabla\Psi_{\text{splint}}\|$. This gradient represents the steepness of the artificial potential introduced by the static molecular brace, not mechanical work from an active motor. Once the trajectory enters the target neighborhood, the residual gradient reflects the static potential's response to continuing stochastic perturbations.

4.4 Geometric Confinement within the Kinematic Tether Limit

Panel D of Figure 1 provides a zoomed-in projection of the conformation space near X^*. The post-intervention trajectory is shown to remain confined within the projected tether boundary. Whenever multidimensional thermal noise attempts to drive the coarse-grained conformation beyond the kinematic tether limit, the projected dynamics return the state to the admissible domain. This behavior illustrates the reflected-SDE confinement result: stochastic excursions are bounded by the tether radius. The simulation therefore supports robust finite-radius stabilization, rather than literal elimination of Brownian motion or absolute control over the full apoptotic pathway.

5 Conclusion

This work proposes a mathematical framework for modeling chrysene-based molecular splinting as robust geometric confinement of stochastic apoptotic target conformations. The Entropic Strain Tensor converts conformational deviation into a quadratic strain measure, while an H_∞-inspired minimax formulation provides a design-stage principle for selecting static potentials that reduce worst-case conformational strain. Because a synthesized molecular brace is passive, the admissible physical intervention is restricted to static conservative vector fields or hard geometric constraints, not arbitrary time-dependent feedback.

The central mathematical result is finite-radius confinement. Under a stabilizing splinting potential, the expected strain can be bounded by a stochastic Lyapunov residual term. Under a reflected-SDE hard-boundary idealization, the pathwise strain is bounded by the square of the Kinematic Tether Limit:

$$\text{Tr}(E_{\text{drift}}(t)) \leq r_{\text{tol}}^2.$$

For a graph of constrained coordinates, the global strain satisfies

$$\text{Tr}(E_{\text{global}}(t)) \leq \sum_{i \in V} r_{\text{tol},i}^2.$$

Exact zero strain occurs only in the singular mathematical limit where all tether radii vanish. In physically realizable molecular systems, the correct interpretation is robust bounded confinement rather than literal elimination of Brownian motion.

Within this revised interpretation, the Chrysene Formalism offers a possible theoretical route from probabilistic ligand binding toward geometry-driven conformational stabilization. The next stage of development would require explicit molecular models connecting scaffold geometry to target binding coordinates, quantitative estimates of tether stiffness, and experimental or computational validation of target-specific conformational confinement.

References

[BB95] Tamer Başar and Pierre Bernhard. *H_∞-Optimal Control and Related Minimax Design Problems: A Dynamic Game Approach*. Birkhäuser Boston, 2nd edition, 1995.

[Kha12] Rafail Khasminskii. *Stochastic Stability of Differential Equations*. Springer Berlin Heidelberg, 2nd edition, 2012.

[KM02] Martin Karplus and J. Andrew McCammon. Molecular dynamics simulations of biomolecules. *Nature Structural Biology*, 9:646–652, 2002.

[LL16] Sampath P. Leelananda and Steffen Lindert. Computational methods in drug discovery. *Beilstein Journal of Organic Chemistry*, 12:2694–2718, 2016.

[LS84] Pierre-Louis Lions and Alain-Sol Sznitman. Stochastic differential equations with reflecting boundary conditions. *Communications on Pure and Applied Mathematics*, 37(4):511–537, 1984.

[Sch26a] Charles D. Schaper. *Designing Therapeutics with The Chrysene Formalism: Functorial Mappings in Protein Synthesis and Molecular Pharmacology*. Schaper Systems Press, San Francisco, CA, 2026. ISBN: 979-8-950371-10-3.

[Sch26b] Charles D. Schaper. *Medicine in the Chrysene Topos: Struc- tural Containment and the Multivariate Regulation of Biological Networks*. Schaper Systems Press, San Francisco, CA, 2026. ISBN: 979-8-950371-01-1.

[Sch26c] Charles D. Schaper. *Operadic Topoi over the Chrysene Tensor Space: The Algebraic Geometry of Categorical Containment and Clinical Logic*. Schaper Systems Press, San Francisco, CA, 2026. ISBN: 979-8-950371-05-9.

[TO10] Oleg Trott and Arthur J. Olson. AutoDock Vina: improving the speed and accuracy of docking with a new scoring function, efficient optimization, and multithreading. *Journal of Computational Chemistry*, 31(2):455–461, 2010.